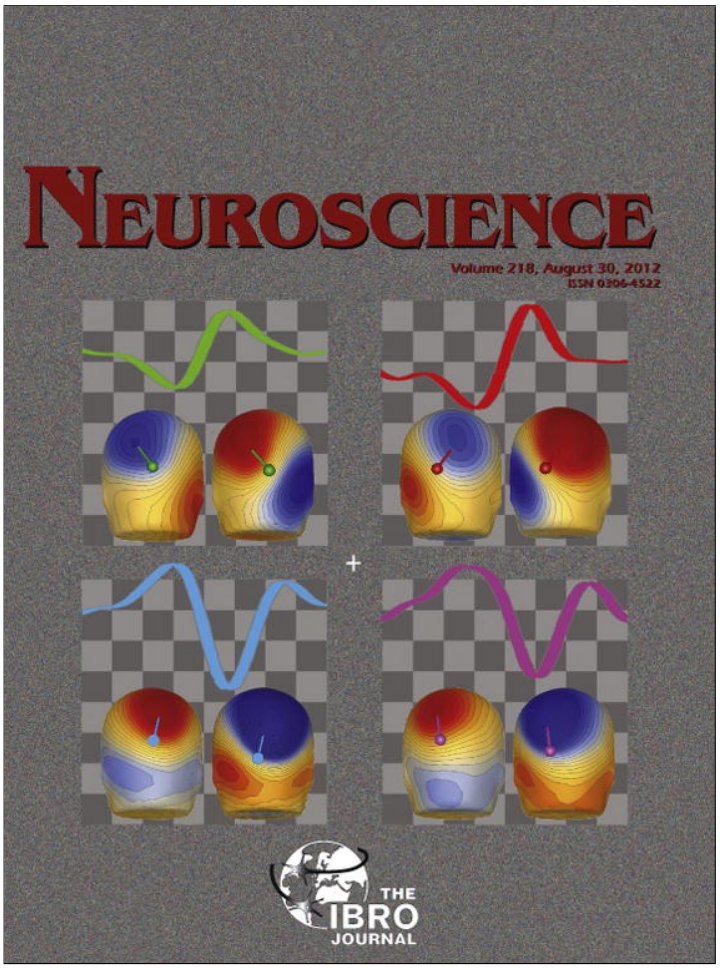

Neuroscience 218 (2012) 226–234

GENERATION OF THE VESPA RESPONSE TO RAPID CONTRAST FLUCTUATIONS IS DOMINATED BY STRIATE CORTEX: EVIDENCE FROM RETINOTOPIC MAPPING

E. C. LALOR, [a,b,c,d]* **S. P. KELLY** [a,e] **AND J. J. FOXE** [a,d,f]

[a] *The Cognitive Neurophysiology Laboratory, Nathan S. Kline Institute for Psychiatric Research, 140 Old Orangeburg Road, Orangeburg, NY 10962, USA*

[b] *School of Engineering, Trinity College Dublin, Dublin 2, Ireland*

[c] *Trinity Centre for Bioengineering, Trinity College Dublin, Dublin 2, Ireland*

[d] *Trinity College Institute of Neuroscience, Trinity College Dublin, Dublin 2, Ireland*

[e] *Department of Biomedical Engineering, City College of New York, New York, NY 10032, USA*

[f] *The Cognitive Neurophysiology Laboratory, Children's Evaluation and Rehabilitation Center, Departments of Pediatrics and Neuroscience, Albert Einstein College of Medicine, Van Etten Building – Wing 1C, 1225 Morris Park Avenue, Bronx, NY 10461, USA*

Abstract—The VESPA (visual-evoked spread spectrum analysis) method derives an impulse response function of the visual system from scalp electroencephalographic (EEG) data using the controlled modulation of some feature of a visual stimulus. Recent research using VESPA responses to modulations of stimulus *contrast* has provided new insights into both early visual attention mechanisms and the specificity of visual-processing deficits in schizophrenia. To allow a fuller interpretation of these and future findings, it is necessary to further characterize the VESPA in terms of its underlying cortical generators. To that end, we here examine spatio-temporal variations in the components of the VESPA as a function of stimulus location. We found that the first two VESPA components (C1/P1) each have a posterior dorsal midline focus and reverse in polarity across the horizontal meridian, consistent with retinotopic projections to calcarine cortex (V1) for the stimulus locations tested. Furthermore, the focal scalp topography of the VESPA was strikingly constant across the entire C1–P1 timeframe (50–120 ms) for each stimulus location, with negligible global scalp activity visible at the zero-crossing dividing the two. This indicates a common focal source underpinning both components, which was further supported by a significant correlation between C1 and P1 amplitudes across subjects ($r = 0.54$; $p < 0.05$). These results, along with factors implicit in the method of derivation of the contrast-VESPA, lead us to conclude that these responses are dominated by activity from striate cortex. We discuss the implications of this finding for previous and future research using the VESPA.

Key words: EEG, visual-evoked potential, VESPA, V1, striate cortex.

INTRODUCTION

The visual-evoked potential (VEP) technique is a widely used and extremely valuable tool in both research and clinical settings for the evaluation of sensory and perceptual processing (Celesia and Peachey, 2005). It is typically derived by averaging epochs of electroencephalography (EEG) around repeated, discrete presentations of a visual stimulus. Because of its widespread use, understanding the VEP's cortical generators is of major importance. Over the past few years, we have introduced and utilized a novel visual-evoked potential that we have termed the i.e., VESPA (visual-evoked spread spectrum analysis; Lalor et al., 2006) response. Unlike the VEP, this response is obtained using continuous stochastic modulation of a visual stimulus feature and regression of the concurrently recorded EEG (see Experiment procedures). Studies using the VESPA have provided valuable new insight into mechanisms of visual spatial attention (Lalor et al., 2007; Frey et al., 2010) as well as into the highly specific nature of visual processing deficits in schizophrenia (Lalor et al., 2008).

The temporal progression of the VESPA derived at midline occipital scalp sites is very similar to that of the averaged VEP for foveal stimuli. However, while the earliest component ("C1") of the two responses displays a similar spatial distribution, the VESPA response is much more spatially delimited than the VEP for later components (Lalor et al., 2006). In particular, the second component of the VEP, known as the P1 and typically peaking between 95 and 115 ms, displays a marked bilateral spread, while the VESPA P1 is tightly focused over the midline, much like the C1 that is induced under both methods. Given the utility of the VESPA in studying cognitive and sensory processing in healthy individuals and in psychiatric disorders, it is critical to further characterize the response in terms of its cortical origins.

One potentially useful approach to tackling this question is to examine spatio-temporal variations of the VESPA components as a function of the retinal location of

*Correspondence to: E. C. Lalor, Trinity College Institute of Neuroscience, Trinity College Dublin, Dublin 2, Ireland. Tel: +353-1-8961743; fax: +353-1-6772442.
E-mail address: edlalor@tcd. ie (E. C. Lalor).

Abbreviations: EEG, electroencephalography; MVEP, multi-focal VEP; SVD, singular value decomposition; VEP, visual-evoked potential; V-ESPA, visual-evoked spread spectrum analysis.

0306-4522/12 $36.00
http://dx.doi.org/10.1016/j.neuroscience.2012.05.067

the evoking stimulus. This approach has been commonly used to assess the cortical origins of the averaged VEP (Jeffreys and Axford, 1972; Butler et al., 1987; Gomez-Gonzalez et al., 1994; Clark et al., 1995; Seki et al., 1996; Slotnick et al., 1999; Di Russo et al., 2002, 2005). Such studies have revealed that the initial C1 (peaking 65–90 ms) exhibits changes in scalp distribution as a function of visual field location that are highly consistent with retinal representation within primary visual cortex (V1), which lies along the banks and within the depths of the calcarine fissure (Polyak, 1957; Jeffreys and Axford, 1972; see Butler et al., 1987). One aspect of the so-called "cruciform model" that emerged from these observations was that the C1 evoked by a stimulus presented within either upper field quadrant (centered away from the vertical meridian which projects outside the calcarine) is negative in polarity over posterior midline scalp, whereas the mirrored locations in the lower field evoke a positive C1 (e.g., Di Russo et al., 2002).

While the vast majority of studies on this issue have argued for a V1 source of the C1 (see Di Russo et al., 2002), it has been pointed out that other visual regions are likely to contribute after the initial 10–15 ms (Foxe and Simpson, 2002). Some studies have gone even further, specifically suggesting contributions from V2 and/or V3 in C1 generation even from its onset (Hagler et al., 2009; Ales et al., 2010b, but see Kelly et al., 2012).

With these considerations in mind, the present study seeks to use stimuli at multiple locations to examine spatio-temporal variations in the VESPA in combination with source analysis. Our data suggest a dominant role for generators in the primary visual cortex for both the first (VESPA C1) and second (VESPA P1) components. These findings complement another recent paper from our group that demonstrates correlations among the VESPA C1, VESPA P1 and VEP C1 but not the VEP P1 (Murphy et al., 2012).

EXPERIMENTAL PROCEDURES

Subjects

Written informed consent was obtained from 15 healthy subjects. This group comprised paid volunteers aged between 18 and 40 years. All subjects reported normal or corrected-to-normal vision. The experiment was undertaken in accordance with the Declaration of Helsinki and was approved by the Institutional Review Board of the Nathan Kline Institute.

Stimuli and procedure

Four checkerboard-patterns each subtending visual angles of 5.25° vertically and horizontally and with equal numbers of light and dark checks were used throughout this study. As in Lalor et al. (2006), the refresh rate of the monitor was set to 60 Hz and on every refresh the contrast of each checkerboard pattern was modulated by a stochastic waveform which had its power distributed uniformly between 0 and 30 Hz. The contrast of each checkerboard was modulated using a different stochastic signal, each of which was uncorrelated with every other signal. One checkerboard was located in each quadrant centered at ±6.5° lateral and above or below a centrally presented crosshair that subtended angles of 0.5° both horizontally and vertically (Fig. 1).

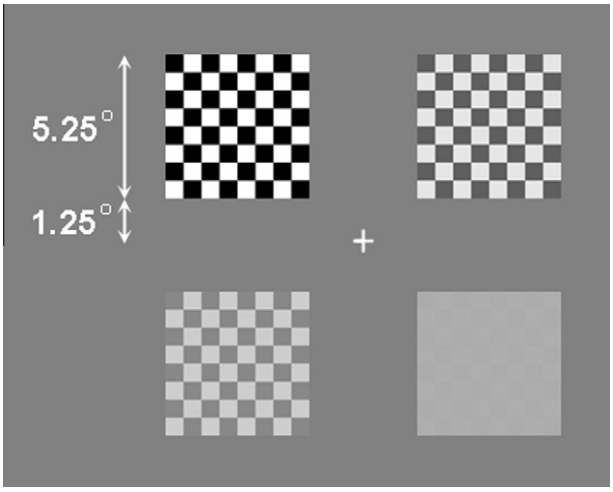

Fig. 1. Setup used throughout. Subjects were instructed to maintain fixation on the central crosshair at all times while the checkerboards were each modulated by a different stochastic signal.

Each subject underwent 15 runs of 120 s each. Subjects were instructed to maintain visual fixation on the crosshair at the center of the screen for the duration of each run and to keep the number of eye-blinks and all other motor activity to a minimum.

EEG acquisition and analysis

EEG data were recorded from 168 electrode positions referenced to location Fz, filtered over the range 0–134 Hz and digitized at a rate of 512 Hz using the BioSemi Active Two system. Subsequently, the EEG was digitally filtered with a high-pass filter with passband above 2 Hz and −60 dB response at 1 Hz and a low-pass filter with 0–35 Hz passband and −50 dB response at 45 Hz.

The VESPA is an estimate of the linear impulse response of the visual system (Lalor et al., 2006). It is based on the assumption that the EEG response to a stimulus, whose luminance or contrast is rapidly modulated by a stochastic signal, consists of a convolution of that signal with an unknown impulse response. Given the known stimulus signal and the measured EEG, this impulse response, i.e., the VESPA, can be estimated using the method of linear least squares. Because the four stimulus signals were uncorrelated it was possible to obtain four VESPA responses simultaneously from one EEG recording. In the present study VESPAs were measured using a sliding window of 500 ms of data starting 100 ms pre-stimulus. VESPAs were calculated for each 120 s run and then averaged across runs. On the basis that no VESPA responses were visible for any location for one subject, the data for that subject were not included in the analysis that follows.

RESULTS

VESPA responses from midline parietal location Pz averaged over 14 subjects and corresponding to each of the four stimuli are plotted in Fig. 2. The first two components peaking at around 75 and 105 ms, respectively, can be seen to invert in polarity for upper versus lower visual field stimuli. The responses to stimuli in the lower visual field also display a third, small positive component at around 140 ms. No corresponding negative component at this time is evident in response to the upper visual field stimuli. Despite the fact that the first two components *both* invert

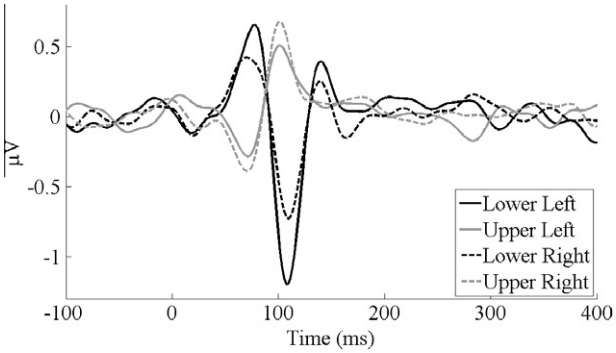

Fig. 2. Plot of the grand average VESPA for each stimulus location at midline parietal electrode location Pz.

in polarity, for convenience we will hereafter refer to them as the C1 and P1 components of the VESPA respectively, in keeping with the labels given to the first two components of the VEP.

A fuller picture of the VESPA responses to each stimulus location can be seen in Fig. 3, which shows the scalp distribution of each response as it evolves over time. For lower field stimuli, the positive pole of the C1 component was focused over occipitoparietal scalp slightly contralateral to the midline. For upper field stimuli, this component reversed in polarity and was focused over occipitoparietal scalp slightly ipsilateral to the midline. Interestingly, the C1, both for upper and lower visual stimuli appears to retain its distribution on the scalp throughout the onset and offset of the component. At some point between 85 and 95 ms global scalp activity becomes negligible on transition to the second component, the P1. For each of the stimulus locations the P1 displays a strikingly similar scalp distribution to the corresponding C1, but with a reversed polarity. Again the distribution of the P1 component across the scalp appears to remain stable as it rises and falls. The later positive component, evident in the responses to the lower visual field stimuli between around 130 and 150 ms, displays a spatially focused distribution that is similar to those of the preceding two components.

To statistically test for any dissimilarity between the C1 and P1 scalp distributions, we used the ‘‘topographic ANOVA’’ or TANOVA method (Lehmann and Skrandies, 1980), which is a non-parametric test of topographic dissimilarity. The C1 and P1 components were defined as the average values at every electrode over the intervals 70–85 and 95–110 ms, respectively. We compared the topographic distribution of the C1 component for each stimulus location with that of the *inverted* P1 component at the same location. For each of the locations, the distributions of the C1 and (inverted) P1 components were found to be not significantly different: upper-left, $p = 0.76$; upper-right, $p = 0.91$; lower-left, $p = 0.35$; lower-right $p = 0.46$. (By way of comparison, a TANOVA conducted on the obviously different P1 topographies for upper-left and upper-right stimuli revealed a significant difference with $p = 0.018$).

In order to further examine the similarities between the C1 and P1 components of the VESPA, we wished to assess if their amplitudes were correlated across subjects.

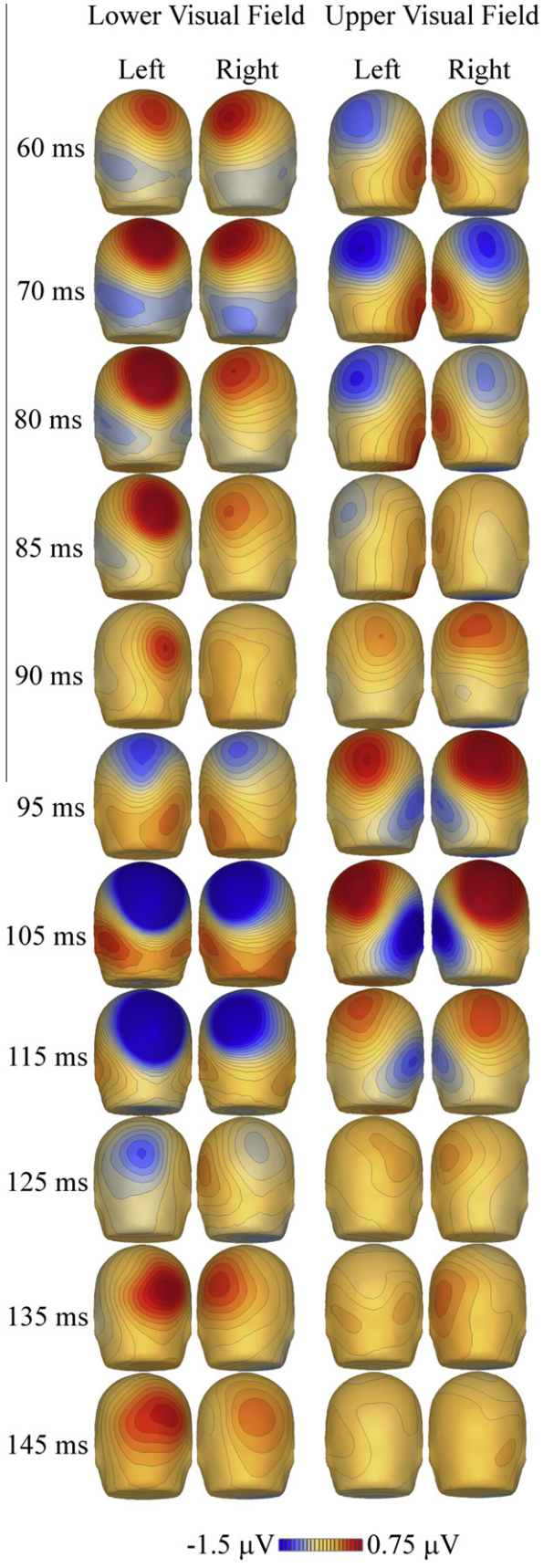

Fig. 3. Topographic distribution of the VESPA obtained to each stimulus position (lower-left, lower-right, upper-left and upper-right) at 70 ms (C1) and 105 ms (P1).

To that end, we determined values for the amplitudes of the C1 and P1 components for each subject and each stimulus location. Because the topographies varied with stimulus position, we chose to measure the C1 and P1 components at the electrode closest to the focus of the grand average data shown in Fig. 3. Given their topographical similarity, one right parietal electrode satisfied this criterion for both the lower left and upper right stimuli. Similarly one left parietal electrode was used for the upper left and lower right stimuli. We determined the peak amplitude of the C1 and P1 components for each stimulus and each subject by detecting the appropriate extremum value (e.g., minimum for upper field C1) in the intervals 70–85 and 95–120 ms respectively at the relevant electrode. In order to improve our signal to noise ratio, we then averaged our amplitude measures over all four stimulus positions with appropriate sign inversions to equate polarity, giving us a single C1 and single P1 amplitude value for each of our 14 subjects. A Pearson's correlation test between the C1 amplitude and inverted P1 amplitude revealed that these amplitudes were significantly correlated across subjects ($r = 0.5439$, $p = 0.04$).

Based on these similarities in scalp distribution and amplitude, it seemed plausible that the C1 and P1 components for each VESPA may have a common cortical generator. Furthermore, the extremely focal distribution of the activity on the scalp (e.g., at 70 and 105 ms), was strongly suggestive of a unitary, localized cortical generator. We therefore attempted to model our responses with a single dipole using the BESA software package (http://www.besa.de). Specifically, we attempted to fit a single dipole to the C1 component and, independently, a single dipole to the (inverted) P1 component for the VESPA corresponding to each stimulus location. For this source analysis, we once again defined the C1 and P1 components based on the activity in the intervals 70–85 and 95–110 ms respectively. Table 1 presents the outcome of this analysis. Single dipoles in early visual cortex accounted very well for the data, with more than 90% of the variance explained by these simple models for all components and locations. Clearly the location and orientation of the best-fitting single dipole to the C1 and P1 components were nearly identical for each VESPA response. In addition, the best-fitting single dipole was located in primary visual cortex (Brodmann area 17) for three of the four stimulus locations. The best-fitting dipole for the upper-left stimulus was localized to a point just outside primary visual cortex (Brodmann area 18), within a reasonable distance from the border. Fixing the source to a nearby location in area 17 resulted in only a 0.2% drop in explained variance (95.0–94.8%), indicating that the source for this location is likely to accord with the other three.

The best-fitting dipoles for each component and location are overlaid on the MNI brain (Collins et al., 1998) in Fig. 4. The similarity between the best fit models of the C1 and the (inverted) P1 are evident. Notably, for both components, the dipoles corresponding to the left- and right-field stimuli are located in the contralateral hemisphere. Furthermore, for both components, but particularly the C1, the dipoles corresponding to the lower-field stimuli are located dorsal to those corresponding to the upper-field stimuli. This crossover of sources is highly consistent with the retinotopic structure within calcarine fissure.

In order to further assess the possibility of a single source generating both the C1 and P1 components for each location, we sought to quantify the dimensionality of our VESPA responses. Using a method similar to that performed by Zhang and Hood (2004), we performed a singular value decomposition (SVD), or principal component analysis (PCA) on the 160 channel VESPA response. We did this separately for the responses from each of the four locations because of their divergent topographic distributions and the differing locations of their putative sources (Table 1). We tested two time intervals: one that included just the C1 and P1 components (45 EEG samples covering 45–130 ms) and one that also included the later positive component seen for the lower field stimuli (60 samples cover 45–160 ms). Thus, we carried out SVD on four matrices with dimensions 160 channels $\times$ 45 samples and on four matrices with dimensions 160 channels $\times$ 60 samples. The percentage of variance in the data that could be explained by one or two principal components for each of the four locations, for both intervals of interest is presented in Table 2.

The high percentage of the variance explained by just one principal component across the entire timeframe of the C1 and P1 components strongly suggests a dominant role for a single underlying source. Having said that, it is

Table 1. Talairach coordinates and orientation of independent single dipole fits to the C1 and P1 components of the VESPAs obtained to stimuli in each of the four quadrants of the visual field. The corresponding Brodmann area and the amount of variance explained by each of these single dipole models is also provided

Stimulus location	Component	Talairach coordinates			Orientation			Explained variance (%)
		x	*y*	*z*	*x*	*y*	*z*	
Upper left	C1	7	−77	5	−0.5	−0.5	0.7	95.0
	P1	10	−78	4	−0.6	−0.4	0.7	96.5
Upper right	C1	−16	−81	4	0.5	−0.6	0.7	94.6
	P1	−17	−76	6	0.5	−0.5	0.7	97.6
Lower left	C1	5	−82	11	0.2	−0.6	0.8	93.4
	P1	8	−86	6	0.2	−0.7	0.7	94.4
Lower right	C1	−15	−72	12	−0.1	−0.5	0.9	93.4
	P1	−21	−81	7	0.0	−0.6	0.8	92.9

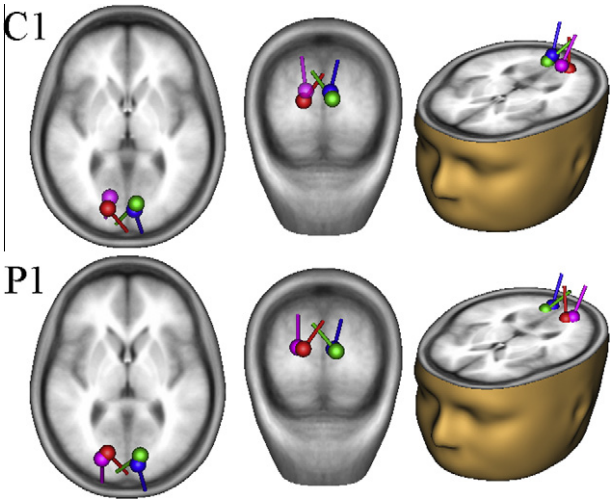

Fig. 4. Location and orientation of single dipole models fit to the C1 (top row) and the (inverted) P1 (bottom row) components. Blue – lower left stimulus, pink – lower right stimulus, green – upper left stimulus, red – upper right stimulus. (For interpretation of the references to color in this figure legend, the reader is referred to the web version of this article.)

clear that the addition of a second principal component explains an additional portion of the remaining variance, indicating that there is likely to be lesser contributions from other sources, e.g., V2 and V3.

Finally, following Di Russo et al. (2005), we performed an additional analysis to compare the peak latencies of the response components when obtained to upper versus lower field stimuli. As with the results of that study, we found no difference in the latencies of the earliest component (our C1) when obtained to upper versus lower field stimuli (paired *t*-test $p = 0.57$). However, we did find a difference in the peak latency of the P1 component when obtained to upper versus lower field stimuli (paired *t*-test $p = 0.035$). The mean P1 peak latency was 103.4 ms for upper field stimuli and 108.8 ms for lower field stimuli.

DISCUSSION

We have obtained VESPA responses simultaneously to contrast modulations of stationary stimuli located in each of the four quadrants of the visual field. Each of these responses displays a focused, spatially restricted scalp distribution that remains remarkably stable over its entire duration, even across successive positive and negative components. In addition, the responses to upper and lower visual field stimuli have opposing polarities across the full processing timeframe of their first two components, with responses to upper field stimuli displaying a slight ipsilateral bias on the scalp and responses to lower field stimuli displaying a slight contralateral bias. Finally, the amplitudes of the first two components are found to be correlated across subjects when averaged over the four stimulus positions.

These findings suggest that the first two components of the VESPA share the same neural generators. Further, we contend that the entirety of the VESPA response (as evoked with this particular stimulus) is dominated by activity from calcarine cortex (V1). This proposal is well supported by inverse source estimations, which resulted in unconstrained fitting of single equivalent dipoles in or very close to calcarine cortex for all quadrants in a spatial configuration that is consistent with its (admittedly idealized) retinotopic organization.

It was recently pointed out that activation of visual areas V2 and V3 by upper and lower field stimuli can result in polarity inversion of the activity on the scalp, as is the case for V1 (Ales et al., 2010b). It is thus necessary for us to provide further arguments for our interpretation of a dominant (although, not exclusive) role for V1. One particular reason for our conclusion is based on the nature of the stimulus used in this study. Specifically, our stimulus involved contrast modulation of a checkerboard between 0% and 100% by a Gaussian random process with a zero-point corresponding to the mid-point of the range (i.e., 50% contrast) and with a scaling that allowed ± 3 standard deviations within the range. As such, the stimulus spends $>97\%$ of its time above 16% contrast, and $>84\%$ of its time above 33% contrast. Given the assumption of a linear relationship between contrast and EEG in the VESPA derivation, this means that the response will be dominated by activity from visual areas whose contrast-response functions are relatively linear at these high contrasts. A number of previous studies investigating contrast response functions in different visual areas lead us to infer a dominant role for V1. For example, fMRI contrast responses in human V1 have been shown to vary continuously and monotonically over contrasts greater than 6%, where responses from V3 and MT essentially saturate above 6% (Tootell et al., 1995). Thus, it has been suggested that one can selectively activate V1 (relative to V3/MT, at least), by using stimuli with contrasts greater than 6% (Tootell et al., 1998). In addition, this same study showed much less activation in V2 than in V1 for such stimuli. More recently, lower saturation levels were seen for V2 population responses in macaques using optical imaging, with V2 contrast response functions beginning to flatten around contrast levels of 20–40% and saturating at $>40\%$ contrast (Lu and Roe, 2007). Similarly, single unit recordings in macaques have

Table 2. Percentage of variance explained by one or two principal components for each of the four stimulus locations, for two intervals that include the C1 and P1 components

Interval	Number of principal components	Upper left	Upper right	Lower left	Lower right
45–130 ms (C1–P1)	1	90.1	92.4	93.4	91.1
	2	96.4	97.8	98.2	95.4
45–160 ms	1	85.8	85.4	91.5	85.9
	2	94.8	96.0	97.9	91.9

shown a gradual reduction in the semi-saturation contrast as one progresses up the visual system (V1 – Sclar et al., 1990; V2 – Levitt et al., 1994; V3 – Gegenfurtner et al., 1997; MT – Sclar et al., 1990). All of these studies suggest that the majority of frame-by-frame stimulus contrast transitions made by the stimuli in the present study are likely to be among levels exceeding the saturation point in extrastriate cells, and so these cells would not be expected to contribute significantly to the scalp response.

In order to provide an illustration for the above reasoning, we conducted a simulation on how differing contrast response curves might affect the estimated linear VESPA. We first generated four response curves using an equation for fMRI contrast-response functions described by Boynton et al. (1999) where each of these curves was designed to saturate at a different contrast level. We then generated a random Gaussian ''contrast modulation'' signal exactly like those used in our EEG experiment. We used this modulation signal to generate four simulated EEG traces by convolving the contrast modulation signals with a hypothetical impulse response function, where the contrast modulation signals were scaled at each contrast level according to the four contrast response curves shown in Fig. 5a. We then estimated the original impulse response function, i.e., the VESPA response using our standard linear regression analysis. As can be seen in Fig. 5b, the acquired VESPA responses diminish as the semi-saturation point of the corresponding contrast response function is decreased.

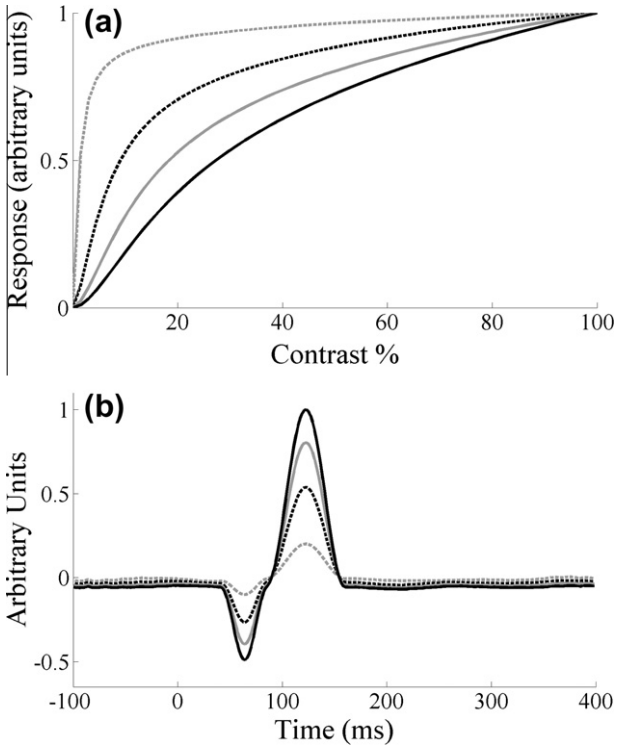

Fig. 5. Effect of contrast response saturation on the linear VESPA. (a) Hypothetical contrast response curves for different visual areas, each with a different saturation level. (b) The linearly VESPA responses estimated based on EEG that was simulated using the contrast response curves in (a).

It is useful to also consider the VESPA stimulus in relation to those used in other rapid visual response estimation techniques based on reverse correlation, such as the multi-focal VEP (MVEP) technique (Baseler et al., 1994). Although earlier studies claimed that the MVEP was generated solely in V1 (Baseler et al., 1994; Slotnick et al., 1999; Fortune and Hood, 2003; James, 2003; Zhang and Hood, 2004; Klistorner et al., 2005; Maddess et al., 2006), Ales et al. (2010b) recently assumed identical current source density in V1 and V2 when modeling the scalp activity resulting from a multi-focal stimulus. As pointed out above, however, the functional distinctions between cells in different visual areas would predict different relative contributions from these areas depending on the stimulus. Given the particular contrast dynamics of our VESPA stimulus, it is likely that differences in the relative response contributions from V1 and V2 will be even more pronounced, with V1 activity being even more dominant than in the case of the multifocal VEP.

A second argument can be made for a striate cortical source for the VESPA based on the constancy of its highly localized topographical distribution across the timeframe encompassing both the C1 and P1. Foxe and Simpson (2002) have suggested that, because of differences in onset timing between V1 and V2, one can rely on the focused topographical distribution of the earliest part of the C1 component as a marker for V1. In critiquing this approach, Ales et al. (2010b) have pointed out that focal scalp topographies at early latencies in response to small stimuli could arise from summed sources in V1, V2 and V3 that are compact and close together in three dimensions. They have also suggested that V1 and V2 onset at essentially the same time (Ales et al., 2010a). If this were true, then the VESPA could be generated by simultaneously onsetting activations in V1 and V2. However, the fact that the VESPA response remains topographically focused over its entire duration and is almost negligible on the scalp at the cross-over timepoint between the C1 and P1 components, which are correlated in amplitude, counts against this notion. Even if V1 and V2 did onset at the same time, it seems highly unlikely that they would be located and oriented almost identically in the brain. It seems even more unlikely that they would follow precisely the same temporal activation profile over the extended C1–P1 timeframe so that neither area is expressed at the zero-crossing.

In any case, the contention that V1 and V2 onset at the same time is not supported by non-human primate intracranial work. All studies examining the relative timing of response onset in visual areas (Schmolesky et al., 1998; Schroeder et al., 1998; Nowak et al., 1999; Mehta et al., 2000) have clearly demonstrated that V1 becomes active before V2, in keeping with the known connectivity in the hierarchically organized visual system. Another modeling study using very similar processing steps showed that V1 becomes active 13 ms before V2 (Hagler et al., 2009). This 13 ms lag is far from negligible and accords well with both monkey data (Schroeder et al., 1998; Nowak et al., 1999) and with the conclusions of Foxe and Simpson (2002). It should be noted, however, that Hagler et al. (2009) did find a similar onset time for their

estimated V3 response as their estimated V1 response. As with the Ales et al. (2010a) study, however, it seems unlikely that a V1 source and V3 source would both be located and oriented almost identically in the brain and would follow precisely the same temporal activation profile.

Our interpretation of a dominant role for V1 in generating the VESPA C1 and P1 directly follows the reasoning in previous studies of the C1 component of the visual-evoked potential evoked by either pattern-onset stimuli (Clark et al., 1995; Simpson et al., 1995; Di Russo et al., 2002; see also Kelly et al., 2012) or pattern-reversal stimuli (Di Russo et al., 2005). Each of these studies used source localization to complement their analysis of retinotopic scalp distribution in identifying the origin of the C1 as primary visual cortex. In turn, each of these papers has concluded that the earliest component of the visual-evoked potential represents the initial volley of activity from thalamus into V1. Recent work from our group has further shown that the VEP C1 and VESPA C1 amplitudes are highly correlated across subjects providing yet more evidence for a correspondence in their cortical sources (Murphy et al., 2012).

A direct comparison of the VESPA P1 and the VEP P1 is not as straightforward however. The main reason for this is that, since the VESPA is based on our assumption of a simple linear relationship between stimulus contrast and output EEG which, as discussed earlier is likely to return a response dominated by activity from early visual areas. Meanwhile, the VEP, which is typically based on straightforward time-locked averaging in response to a discrete stimulus event, is made up from the complex, nonlinear superposition of activity from multiple visual areas (Schroeder et al., 1998; Foxe and Simpson, 2002). During the time frame of the VEP C1 component, particularly the first 10–15 ms, activity in areas other than primary visual cortex is relatively minimal (Foxe and Simpson, 2002; Foxe et al., 2008). However, at the latency of the P1 component, multiple visual areas are active and contribute concurrently to that component (Clark et al., 1995; Di Russo et al., 2002; Foxe and Simpson, 2002).

Studies using pattern-reversing stimuli have demonstrated that, among the several generative sources of the VEP, is a primary cortical source displaying C1 and P1 components that can both be well modeled by the same dipole (Hatanaka et al., 1997; Nakamura et al., 2000; Di Russo et al., 2005). This source may correspond to our VESPA response. Such a correspondence would suggest the exciting possibility that the VESPA can be used to obtain highly temporally resolved responses from primary visual cortex in relative isolation from concurrent activity in other visual areas.

The data presented in this paper present a number of challenges in terms of interpreting previous results based on the VESPA. In particular, we have previously found attentional modulation of only the P1 component of the VESPA (Lalor et al., 2007; Frey et al., 2010). This begs the question: if the entire VESPA response represents activity from V1, why would an attentional modulation only affect one component? We think there are two possible explanations for this. First, while the VESPA P1 may be dominated by activity from V1, it may also include some lesser contribution from extrastriate cortex – a suggestion that is supported by our SVD analysis – and only this contribution may have been modulated, in accordance with suggestions that extrastriate, but not striate cortex is affected by attention (Clark and Hillyard, 1996). However, it has been shown that V1 activity can be modulated by attention during a reentrant volley from extrastriate cortex (Martínez et al., 1999; Noesselt et al., 2002) and under certain stimulus/task conditions, even in the initial afferent volley (Kelly et al., 2008; Poghosyan and Ioannides, 2008; Rauss et al., 2009). Therefore, the second possibility is that, in the tasks of Lalor et al. (2007) and Frey et al. (2010), the attentional modulations of P1 may in fact have been modulations of V1 activity and that the lack of an attentional modulation of the C1 in these studies may indicate cognitive separability of the two successive processing stages represented by these components in V1. Further work exploring different task demands and using more invasive recording techniques may be needed to address this issue.

Our recent results on visual processing in schizophrenia may also be enlightened to some extent by the current findings. In particular, Lalor et al. (2008) showed that the P1 component of the standard VEP was much reduced in schizophrenia patients when compared with controls, while there was no such difference with the VESPA P1. The simple model of VESPA P1 activity proposed here suggests that it is dominated by activity from V1 whereas the averaged VEP P1 contains contributions from multiple cortical areas. Thus, the dissociation between VESPA and VEP results in comparisons of schizophrenia patients with controls may be due to the insensitivity of the VESPA to cortico-cortical connectivity dysfunction in schizophrenia that is captured by the VEP (see e.g., Kemner et al., 2009). Further work aimed directly at this hypothesis is ongoing.

CONCLUSION

We have shown here that the C1 and P1 components of VESPA reverse in polarity when derived from upper versus lower field stimuli and that the two components share a close correspondence in terms of topographical distribution and amplitude across subjects. Moreover, little else beyond these well-circumscribed components seems to be captured in the VESPA. This is in marked contrast with the standard visual-evoked potential, in which scalp potentials shortly following the initial C1 clearly receive contributions from diverse brain areas and lose their retinotopic specificity. These results, along with evidence from source analysis, suggest that the VESPA is dominated by activity from calcarine cortex with significantly less contribution from extrastriate areas. Thus it may provide a unique window into the activity of very low-level visual cortex in humans, allowing us to build on decades of extensive non-human primate investigations.

Acknowledgments—*This work was supported by grants from the U.S. National Institute of Mental Health (MH065350 and*

MH085322) to J.J. Foxe. Additional salary support was provided through a Fund for Digital Research Programme grant from the Higher Educational Authority of Ireland and a Government of Ireland Postdoctoral Research Fellowship from the Irish Research Council for Science, Engineering and Technology. The authors are grateful to Jennifer Montesi for assistance in gathering the data and to Jeremy Murphy for helpful comments.

REFERENCES

Ales J, Carney T, Klein SA (2010a) The folding fingerprint of visual cortex reveals the timing of human V1 and V2. Neuroimage 49:2494–2502.

Ales JM, Yates JL, Norcia AM (2010b) V1 is not uniquely identified by polarity reversals of responses to upper and lower visual field stimuli. Neuroimage 52:1401–1409.

Baseler HA, Sutter EE, Klein SA, Carney T (1994) The topography of visual evoked response properties across the visual field. Electroencephalogr Clin Neurophysiol 90:65–81.

Boynton GM, Demb JB, Glover GH, Heeger DJ (1999) Neuronal basis of contrast discrimination. Vision Res 39:257–269.

Butler SR, Georgiou GA, Glass A, Hancox RJ, Hopper JM, Smith KR (1987) Cortical generators of the CI component of the pattern-onset visual evoked potential. Electroencephalogr Clin Neurophysiol 68:256–267.

Celesia GG, Peachey NS (2005) Visual evoked potentials and electroretinograms. In: Niedermeyer E, Lopes da Silva F, editors. Electroencephalography: basic principles, clinical applications, and related fields. PA: Lippincott Williams and Wilkins. p. 1017–1044.

Clark VP, Fan S, Hillyard SA (1995) Identification of early visual evoked potential generators by retinotopic and topographic analyses. Hum Brain Mapp 2:170–187.

Clark VP, Hillyard SA (1996) Spatial selective attention affects early extrastriate but not striate components of the visual evoked potential. J Cogn Neurosci 8:387–402.

Collins DL, Zijdenbos A, Kollokian V, Sled JG, Kabani NJ, Holmes CJ, Evans AC (1998) Design and construction of a realistic digital brain phantom. IEEE Trans Med Imag 17:463–468.

Di Russo F, Pitzalis S, Spitoni G, Aprile T, Patria F, Spinelli D, Hillyard SA (2005) Identification of the neural sources of the pattern-reversal VEP. Neuroimage 24:874–886.

Di Russo F, Martínez A, Sereno MI, Pitzalis S, Hillyard SA (2002) Cortical sources of the early components of the visual evoked potential. Hum Brain Mapp 15:95–111.

Fortune B, Hood DC (2003) Conventional pattern-reversal VEPs are not equivalent to summed multifocal VEPs. Invest Ophthalmol Vis Sci 44:1364–1375.

Foxe JJ, Simpson GV (2002) Flow of activation from V1 to frontal cortex in humans. A framework for defining ''early'' visual processing. Exp Brain Res 142:139–150.

Foxe JJ, Strugstad EC, Sehatpour P, Molholm S, Pasieka W, Schroeder CE, McCourt ME (2008) Parvocellular and magnocellular contributions to the initial generators of the visual evoked potential: high-density electrical mapping of the ''C1'' component. Brain Topogr 21:11–21.

Frey HP, Kelly SP, Lalor EC, Foxe JJ (2010) Early spatial attentional modulation of inputs to the fovea. J Neurosci 30:4547–4551.

Gegenfurtner KR, Kiper DC, Levitt JB (1997) Functional properties of neurons in macaque area V3. J Neurophysiol 77:1906–1923.

Gomez-Gonzalez CM, Clark VP, Fan S, Luck SJ, Hillyard SA (1994) Sources of attention-sensitive visual event-related potentials. Brain Topogr 7:41–51.

Hagler Jr DJ, Halgren E, Martinez A, Huang M, Hillyard SA, Dale AM (2009) Source estimates for MEG/EEG visual evoked responses constrained by multiple, retinotopically-mapped stimulus locations. Hum Brain Mapp 30:1290–1309.

Hatanaka K, Nakasato N, Seki K, Kanno A, Mizoi K, Yoshimoto T (1997) Striate cortical generators of the N75, P100 and N145 components localized by pattern-reversal visual evoked magnetic fields. Tohoku J Exp Med 182:9–14.

James AC (2003) The pattern–pulse multifocal visual evoked potential. Invest Ophthalmol Vis Sci 44:879–890.

Jeffreys DA, Axford JG (1972) Source locations of pattern-specific components of human visual evoked potentials: I. Component of striate cortical origin. Exp Brain Res 16:1–21.

Kelly SP, Gomez-Ramirez M, Foxe JJ (2008) Spatial attention modulates initial afferent activity in human primary visual cortex. Cereb Cortex 18:2629–2636.

Kelly SP, Schroeder CE, Lalor EC (2012) What does polarity inversion of extrastriate activity tell us about striate contributions to the early VEP? A comment on Ales et al. (2010). Neuroimage. http://dx.doi.org/10.1016/j.neuroimage.2012.03.081.

Kemner C, Foxe JJ, Tankink JE, Kahn RS, Lamme VA (2009) Abnormal timing of visual feedback processing in young adults with schizophrenia. Neuropsychologia 47:3105–3110.

Klistorner AI, Graham SL, Grigg J, Balachandran C (2005) Objective perimetry using the multifocal visual evoked potential in central visual pathway lesions. Br J Ophthalmol 89:739–744.

Lalor EC, Pearlmutter BA, Reilly RB, McDarby G, Foxe JJ (2006) The VESPA: a method for the rapid estimation of a visual evoked potential. Neuroimage 32:1549–1561.

Lalor EC, Yeap S, Reilly RB, Pearlmutter BA, Foxe JJ (2008) Dissecting the cellular contributions to early visual sensory processing deficits in schizophrenia using the VESPA evoked response. Schizophr Res 98:256–264.

Lalor EC, Kelly SP, Pearlmutter BA, Reilly RB, Foxe JJ (2007) Isolating endogenous visuo-spatial attentional effects using the novel Visual Evoked Spread Spectrum Analysis (VESPA) technique. Eur J Neurosci 26:3536–3542.

Lehmann D, Skrandies W (1980) Reference-free identification of components of checkerboard-evoked multichannel potential fields. Electroencephalogr Clin Neurophysiol 48:609–621.

Levitt JB, Kiper DC, Movshon JA (1994) Receptive fields and functional architecture of macaque V2. J Neurophysiol 71:2517–2542.

Lu HD, Roe AW (2007) Optical imaging of contrast response in macaque monkey V1 and V2. Cereb Cortex 17:2675–2695.

Maddess T, James AC, Ruseckaite R, Bowman EA (2006) Hierarchical decomposition of dichoptic multifocal visual evoked potentials. Vis Neurosci 23:703–712.

Martínez A, Anllo-Vento L, Sereno MI, Frank LR, Buxton RB, Dubowitz DJ, Wong EC, Hinrichs H, Heinze HJ, Hillyard SA (1999) Involvement of striate and extrastriate cortical areas in spatial selective attention: combined evidence from fMRI and event-related potentials. Nat Neurosci 2:364–369.

Mehta AD, Ulbert I, Schroeder CE (2000) Intermodal selective attention in monkeys: I. Distribution and timing of effects across visual areas. Cereb Cortex 10:343–358.

Murphy JW, Kelly SP, Foxe JJ, Lalor EC. (2012). Isolating early cortical generators of visual evoked activity: a systems identification approach. Exp Brain Res. http://dx.doi.org/10.1007/s00221-012-3129-1.

Nakamura M, Kakigi R, Okusa T, Hoshiyama M, Watanabe K (2000) Effects of check size on pattern reversal visual evoked magnetic field and potential. Brain Res 872:77–86.

Noesselt T, Hillyard SA, Woldorff MG, Schoenfeld A, Hagner T, Jancke L, Tempelmann C, Hinrichs H, Heinze HJ (2002) Delayed striate cortical activation during spatial attention. Neuron 35:575–587.

Nowak LG, Munk MH, James AC, Girard P, Bullier J (1999) Cross-correlation study of the temporal interactions between areas V1 and V2 of the macaque monkey. J Neurophysiol 81:1057–1074.

Poghosyan V, Ioannides AA (2008) Attention modulates earliest responses in the primary auditory and visual cortices. Neuron 58:802–813.

Polyak S (1957) The vertebrate visual system. Chicago, IL: University of Chicago Press.

Rauss KS, Pourtois G, Vuilleumier P, Schwartz S (2009) Attentional load modifies early activity in human primary visual cortex. Hum Brain Mapp 30:1723–1733.

Schmolesky MT, Wang Y, Hanes DP, Thompson KG, Leutgeb S, Schall JD, Leventhal AG (1998) Signal timing across the macaque visual system. J Neurophysiol 79:3272–3278.

Schroeder CE, Mehta AD, Givre SJ (1998) A spatiotemporal profile of visual system activation revealed by current source density analysis in the awake macaque. Cereb Cortex 8:575–592.

Sclar G, Maunsell JH, Lennie P (1990) Coding of image contrast in central visual pathways of the macaque monkey. Vision Res 30:1–10.

Seki K, Nakasato N, Fujita S, Hatanaka K, Kawamura T, Kanno A, Yoshimoto T (1996) Neuromagnetic evidence that the P100 component of the pattern reversal visual evoked response originates in the bottom of the calcarine fissure. Electroencephalogr Clin Neurophysiol 100:436–442.

Simpson GV, Foxe JJ, Vaughan Jr HG, Mehta AD, Schroeder CE (1995) Integration of electrophysiological source analyses, MRI and animal models in the study of visual processing and attention. Electroencephalogr Clin Neurophysiol Suppl 44:76–92.

Slotnick SD, Klein SA, Carney T, Sutter E, Dastmalchi S (1999) Using multi-stimulus VEP source localization to obtain a retinotopic map of human primary visual cortex. Electroencephalogr Clin Neurophysiol 110:1793–1800.

Tootell RB, Reppas JB, Kwong KK, Malach R, Born RT, Brady TJ, Rosen BR, Belliveau JW (1995) Functional analysis of human MT and related visual cortical areas using magnetic resonance imaging. J Neurosci 15:3215–3230.

Tootell RB, Hadjikhani NK, Vanduffel W, Liu AK, Mendola JD, Sereno MI, Dale AM (1998) Functional analysis of primary visual cortex (V1) in humans. Proc Natl Acad Sci USA 95:811–817.

Zhang X, Hood DC (2004) A principal component analysis of multifocal pattern reversal VEP. J Vis 4:32–43.

(Accepted 29 May 2012)
(Available online 7 June 2012)